IJL, Issue 2, Vol. 24, 2025
https://doi.org/10.31900/ijl.v24i2.541

Research Article

IRAQI JOURNAL OF LASER

Laser-Ablated Silver Nanoparticles Embedded in P3HT: A Study of Structural and Optical Enhancement

Zainab Jabar Abd Al-Kareem*, Estabraq Talib Abdullah

Department of Physics, College of Science, University of Baghdad, Iraq.
**Email address of the Corresponding author*: zainab.jabbar1804a@sc.uobaghdad.edu.iq

Article history: Received 11 Jun. 2025; Revised 1sept. 2025; Accepted 7 Sept. 2025; Published online 15 Dec. 2025

Abstract: The hole transport layers are critical components of organic conductor-based devices. The metal nanoparticles (NPs) are excellent materials for this purpose. This paper describes the preparation of silver nanoparticles (Ag NPs) using a laser method, which were then mixed with the organic polymer poly(3-hexylthiophene) (P3HT) at different concentrations (0.1, 0.3, and 0.4 wt%). The structural morphology, structure, and optical properties of the new nanocomposite were examined using X-ray diffraction (XRD), field emission scanning electron microscopy (FESEM), atomic force microscopy (AFM), and UV-Vis spectroscopy. The XRD data showed that the created Ag NPs have a crystal structure, with the strongest peaks seen at angles of 38.1°, 44.3°, 64.4°, and 77.4°. The FESEM and AFM tests showed that having more Ag NPs makes the surface rougher and helps spread the nanoparticles better, where the surface roughness increased from 2.04 to 2.46 nm, the mean roughness of the film (Ra) changed from 1.55 to 1.81 nm, and the maximum height of the film (Rmax) ranged from 22.34 to 25.38 nm. The UV-Vis spectroscopy results showed that the material absorbed lighter due to the localized surface plasmon resonance (LSPR) effect, which caused the absorption peaks to move to shorter wavelengths and lowered the optical energy gap from 2.1 eV for pure P3HT to 2 eV with a 0.3 wt% concentration of AgNPs. P3HT nanocomposites with Ag nanoparticles have better structure and optical properties, which make them ideal for organic solar cells and other electronic applications.

Keywords: Poly(3-hexylthiophene), AgNPs, laser ablation, LSPR, nanocomposites, optical properties.

1. Introduction

Organic semiconductors are the most significant category among optoelectronic devices because of their cost-effectiveness, flexibility, and lightweight characteristics [1,2]. The poly (3-hexylthiophene) (P3HT) is the most studied type of conjugated polymer because it can carry electric charge well, stable in different conditions, and can be processed in solution. There are many various applications of these organic polymers, including organic light-emitting diodes (OLEDs), organic solar cells (OSCs), and organic field-effect transistors (OFETs), which have seen extensive utilization [3-5]. P3HT has many advantages, but it is limited because it doesn't absorb much visible light and has average charge carrier mobility [6,7]. To solve these problems, many studies have looked at creating conjugated polymers that include metal nanoparticles (NPs) in the electronic polymer [8]. Metallic Nanoparticles (NPs), especially silver nanoparticles (AgNPs) are of great interest because they have a special effect called localized surface plasmon resonance (LSPR), which improves light absorption and helps move electric charges more easily [9]. The incorporation of AgNPs into P3HT substantially improve the structural, morphological, electrical, and optical properties of the polymer matrix, thereby enhancing device performance. Mustafa and Abdullah (2019) demonstrated that the incorporation of metal nanoparticles into P3HT enhances light absorption and facilitates improved

charge mobility. They studied the effect of P3HT with Al, Ag, and Cu as metallic nanoparticle hybrids. They used laser ablation in liquid (LAL) to synthesize the nanoparticles, and the morphological and structural analysis proved the interaction between P3HT and these nanoparticles [10].

Gan et al. (2025) they demonstrated that employing P3HT in conjunction with silver nanostructures, which increase light, significantly amplified both Raman and fluorescence signals. This phenomenon occurs when light energizes charges in P3HT, which subsequently move to the silver, enhancing the electromagnetic field and amplifying the intensity of both Raman and fluorescence signals [11]. Many of these studies depend on chemical synthesis methods for AgNPs because of their low cost and high efficiency, but these methods suffer from potentially introducing impurities and impacting reproducibility. Despite chemical approaches, laser ablation in liquid (LAL) generates Ag NPs of higher purity, where no capping or stabilizing compounds are required, rendering it an environmentally sustainable method since it gives precise control over NP size and distribution. Due to these features, this method has garnered significant attention for synthesizing nanomaterials [13-15].

Even though LAL-synthesized Ag NPs have many advantages, they haven't been studied much for use in P3HT-based nanomaterials, particularly in chloroform. Consequently, we select the LAL approach, which involves performing laser ablation directly in chloroform (the solvent for dissolving P3HT), resulting in the rapid and uniform dispersion of AgNPs, thereby decreasing agglomeration and enhancing homogeneous incorporation with the polymer. This study aims to employ laser ablation to synthesize Ag NPs for various concentrations (0.1, 0.3, and 0.4 wt%) on the structural, morphological, and optical properties of P3HT's. The motivation of the work, depending on the LAL features, is to utilizing the localized surface plasmon resonance (LSPR) effect of Ag NPs to enhanced light absorption and charge transport in P3HT. By using LAL to make Ag NPs directly in chloroform, we want to improve how well the nanoparticles mix with the polymer and boost the performance of P3HT-based optoelectronic materials.

2. Experimental Parts

2.1. Materials

P3HT, which has a molecular weight of 28000, was used along with schematic 1, and glasses covered with indium tin oxide (ITO) that have a sheet resistance of 12 Ω/sq, supplied by OSSILA Chemical Co. Silver plates with a thickness of 1 mm and a purity of 98.2% were supplied from the local market. Chloroform ($CHCl_3$) with high purity was used as a solvent, which was also provided by OSSILA Chemical Co.

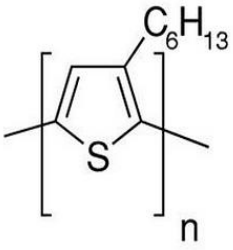

Schematic 1: Poly (3-hexylthiophene) (P3HT).

2.2. Characteristics Technique

Field-effect scanning electron microscopic (FESEM) data were recorded using a Model (Inspect S50). The samples were characterized using AFM to study the topography (Nanosurf Easyscan 2, Switzerland). The X-ray diffraction (XRD) pattern of the prepared AgNPs sample, which was dried in the hot air oven, was recorded at a Model DX-2700BH using CuKα radiation with wavelength = 1.5406 Å. The UV–vis spectroscopy (U-2800, Hitachi double beam, Japan) was used to analyze the prepared samples. The lambda max was measured within the range between 200 and 1100 nm.

2.3. Synthesis of P3HT/Ag NPs Nanocomposites

To dissolve P3HT (20mg), it was added to 1 mL of chloroform, stirred with a magnetic stirrer for 1 h at 60°C, and then put in an ultrasonicator bath for 30 minutes for good polymer stability. First, the silver plate was cleaned with ethanol to remove any contamination. It was added to the peaker (50 ml) containing 20 ml of chloroform, which was used to achieve the affinity with the polymer. To prepare the AgNPs, Q-switched Nd:YAG operating at 1064 nm, and 6 Hz frequency with a energy of 1000 mJ per pulse and a positive lens with a focal lengthof 110mm, which was employed as an ablation source. for 200 shoots was used, Figure.1 shows the laser ablation device. The effective spot size of the laser beam on the metal plate's surface was adjusted between 2.37 mm and 0.4 mm in diameter to enhance the laser fluence. The liquid thickness was adjusted from 2 mm to 14 mm to enhance the shock wave. The liquid thickness is modified by employing various cell dimensions. The quantity of laser blasts administered to the metal target varied from 10 to 80 pulses.

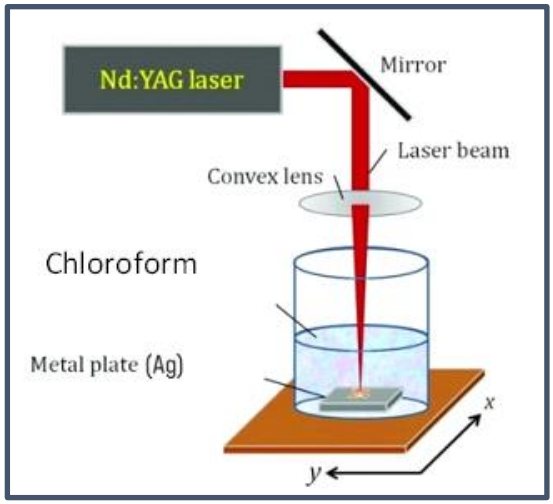

Figure 1: The experimental setup of the preparation of AgNPs by laser device [16].

Fig. 2. The AgNPs that were created were added to a P3HT solution in different amounts (0.1, 0.3, and 0.4 wt%) and mixed for 2 hours at 60°C. They were then placed in an ultrasonic bath for 1 hour. After that, they were applied to ITO substrates using spin coating and heated at 120°C for 10 minutes.

Figure 2*:* The prepared samples of a) pure P3HT, b) 0.1, c)0.3, and d) 0.4 wt% Ag NPs**.**

3. Results and Discussion

The XRD pattern, Fig. 3, shows the crystalline nature of the prepared AgNPs using the laser ablation technique. The important peaks at 2θ values (38.1°, 44.3°, 64.4°, and 77.4°) match the (111), (200), (220), and (311) planes in a face-centred cubic (fcc) silver crystal, according to JCPDS Card No. 04-0783. These results agree with the literature [4,5]. At the same time, the other 2θ values (22.9°, 26.5°, 30.5°, 47°, and 54.3°) may be due to the silver oxide phases (e.g., Ag_2O or AgO) according to the JCPDS No. 41-1104. By using Scherrer equation from the XRD pattern, the mean particle diameter for the Ag NPs can be calculated as follows:

$$D = \frac{k\lambda}{\beta \sin\theta} \quad (1)$$

where λ is the X-ray wavelength, k is the shape constant, βrepresents the full width of the diffraction band (FWHM) for Bragg angle, and θ is the Bragg diffraction angle, respectively. The average crystallite size for Ag NPs was found to be 8 nm. These results satisfy with Rahmah et al. [17] and Kaçuş et al. [18].

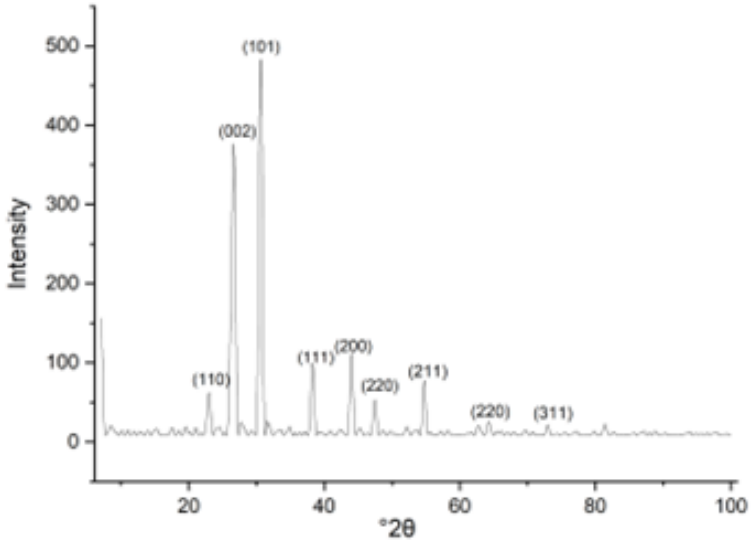

Figure 3: XRD of Ag NPs sample.

To study the morphological structure, only two concentrations of Ag NPs were chosen (0.1 and 0.4 wt%), as shown in Fig. 4a and b. The images show a high tendency for NP agglomeration, especially for higher concentrations. This behavior may be due to the high surface energy of Ag NPs, which makes them aggregate to minimize energy. Also, the preparation method (LAL) doesn't need any surfactants or stabilizers that assist in reducing the aggregation. The uniform size distribution in the P3HT matrix is less broad and broader due to the NPs' agglomeration tendency. This distribution indicates that metallic nanoparticles have a hard time spreading out in the polymer matrix and easily group together into clusters. At 0.1 wt%, the particles tend to clump together, leading to a smaller and less even size range of P3HT, with an average size of about 35 nm. When the concentration of Ag NPs is increased to 0.4 wt%, the silver nanoparticles become more noticeable and spread out better in the polymer matrix, leading to average sizes of about 95 nm. The particle scale distribution illustrates this behaviour in Figure 4. The literature [19,20] reports similar FESEM images of P3HT: Ag NPs. This image shows bright spots on the surface of Ag NPs because of their high atomic number, while the other area appears smooth and darker, indicating the presence of organic P3HT [21].

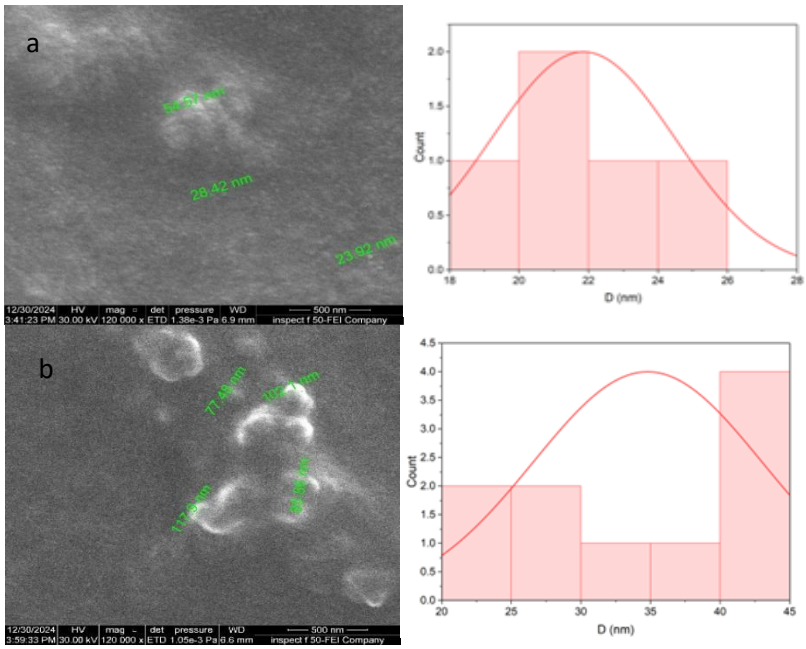

Figure 4: FESEM images and histogram of the particle size distribution of nanoparticles of P3HT (a) with 0.1, and (b) 0.4 wt % Ag NPs.

We appreciate the reviewer for his recommendation. In addition, we extended the discussion to the effects of surface morphology on optical properties, and Figure 5a-b presents 3D AFM plots. The 3D AFM images clearly evidenced that the two parts of the nanostructured P3HT/AgNPs films (Figs. 5a,b), indicating that the plainness of surface for 0. % is fair, and the grain is somewhat spread on the composite surface. With the higher concentration of Ag NPs, the surface roughness is increasing that can result higher probability of agglomeration in the polymer matrix [22,23]. The obtained data indicated that the size of the surface asperities of the film increased from 2.04 to 2.46 nm (Ra) and 1.55-1.81 nm and 22.34-25.38 nm (Ra and Rmax, respectively) of the film, respectively. The enhanced surface roughness may cause enhanced light scattering and absorption which are favourable for the higher generation of excitons.

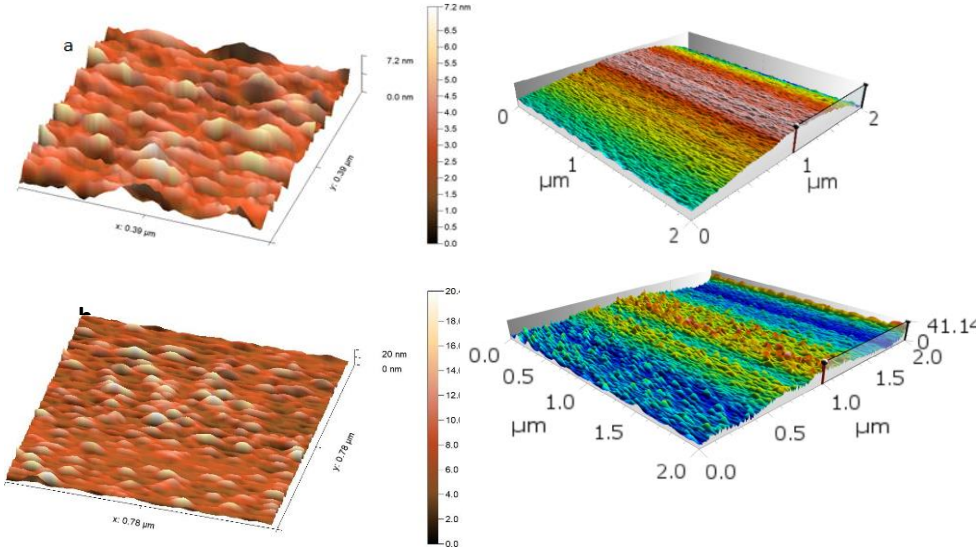

Figure 5: AFM images of P3HT (a) 0.1 wt% AgNPs, and (b) 0.4 wt% AgNPs.

The incorporation of plasmonic NPs into P3HT is an emerging approach to enhancing the optical absorption of polymer matrix. The optical properties of both pure P3HT and nanocomposites of P3HT and AgNPs were examined by the use of UV-Vis spectroscopy. Fig. 6 displays the samples' ultraviolet-visible absorption spectra; as part of the nanoparticle analysis, this included evaluating their absorbance spectra across the wavelength range of 290-600 nm.

Figure 6 indicates the intensity increases with increasing Ag NPs concentration in the nanocomposites, showing that the light absorption improves because of the effects of localized surface plasmon resonance (LSPR). The LSPR of the Ag NPs may couple with the absorption coefficient peak of the P3HT matrix in this case. The increase in the absorption coefficient may be attributed to enhanced light trapping resulting from the incorporation of metallic nanoparticles. The observed increment may also be attributed to the local electrical field enhancement generated by the plasmonic nanoparticles within the polymer matrix [24]. The UV-visible spectrum of the P3HT film showed two peaks at 404 nm and 452 nm, caused by the movement of electrons in the organized structure of the P3HT polymer chains. All exhibited spectra showed a sharp peak near 270–280 nm. This spike might be due to changes in the electrons of the aromatic system or a special effect from AgNPs, which becomes more obvious when there is more Ag. As the concentration of AgNPs increases, the absorption peaks shift to shorter wavelengths, indicating that the electronic structure of P3HT changes because of its interaction or clumping together [25].

Using Beer-Lambert's law: ($\alpha = 2.303A/d$), where A is the absorbance, the absorption coefficient, α, was calculated. Fig. 6 shows the absorption coefficient spectra of the P3HT and P3HT/AgNPs nanocomposites. All samples showed a low absorption in the visible and NIR regions. In the UV range, high absorbance was detected, which is due to the melanin's wide band gap properties [11,12]. In organic semiconductors, the band-gap energy Eg relates to two electron movements: from HOMO (highest occupied molecular orbital) to LUMO (lowest unoccupied molecular orbital), which happen between the molecular orbitals π and π^*. Tauc's method, which uses the formula $\alpha h\upsilon = A(h\upsilon - Eg)1/2$ (where $h\upsilon$ is the energy of the incoming photon), was applied to find the direct band-gap energy by extending the straight line to the photon energy axis. We determined the energy gap of P3HT to be approximately 2.3 eV, which aligns with the literature [13]. The energy gap tends to increase after adding AgNPs to P3HT to form nanocomposites, as shown in Table 1. Crystal regularity also influences these values. The energy gap can be determined using the classical relation for near-edge optical absorption in semiconductors [27]. A slight band gap blue shift (2.35 → 2.38 eV) and the increased absorption intensity imply that the semiconducting nature of P3HT is preserved, as Ag NPs interact plasmonically and alter morphological features of P3HT. this band gap shift may due to enhanced carrier localization, confinement effect, degradation of conjugation length, and Exciton splitting due to the Strong interaction of P3HT with AgNPs.

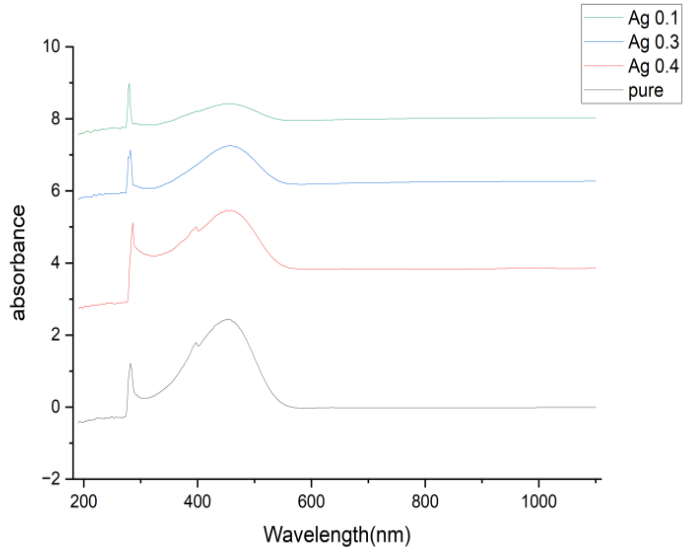

Figure 6: Absorbance spectra for P3HT/Ag NPs nanocomposites.

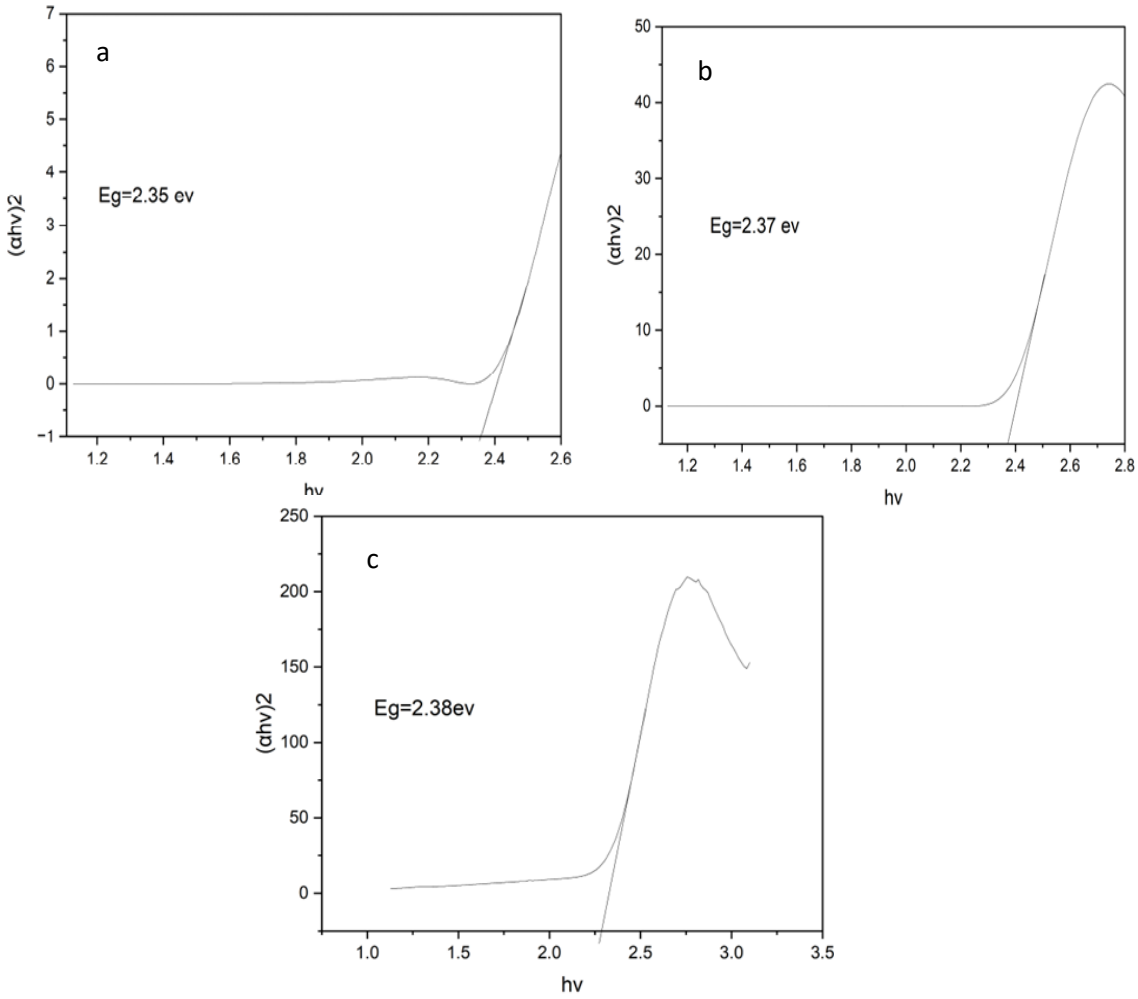

Figure 7: Tauc plot for of P3HT (a) 0.1, (b) 0.3, and (c) 0.4 wt% AgNPs.

Table. 1: The Energy gap values for P3HT/ Ag NPs nanocomposite

Sample	Eg (eV)
Pure P3HT	2.1
0.1	2.35
0.3	2.37
0.4	2.38

4. Conclusions

The preparation of P3HT/Ag nanocomposites exhibits special features in which the silver nanoparticles are made by laser ablation. The surfactant-free Ag NPs, prepared by liquid laser ablation (LAL), with relatively high purity, which minimized any undesired chemical interactions. Structure analysis indicated the existence of Ag NPs crystallites (~9 nm) in a face-centered cubic (fcc) shape. Meanwhile, FESEM results demonstrated the occurrence of regulated agglomerates due to the particle density and polymer attraction. Optical analysis indicated that Ag NPs were able to modulate the intensity of P3HT absorption and emission

spectra, indicating a possible plasmonic effect and excitonic interactions, for example, at the optimized concentrations. These results indicate that the nanocomposite structure and optical properties can be controlled for applications in optoelectronic devices, such as organic solar cells or photodetectors.

References

[1] Q. Zhang, W. Hu, H. Sirringhaus, and K. Müllen, "Recent progress in emerging organic semiconductors", Adv. Mater., 34, 2108701 (2022). DOI: 10.1002/adma.202108701
[2] K. N. Subedi, A. Al-Shadeedi, and B. Lüssem, "Stability of organic permeable base transistors", Appl. Phys. Lett., 115, 193301 (2019). DOI: 10.1063/1.5125233
[3] H. A. Abbas, W. C. Koubaa, and E. T. Abdullah, "Synthesis, characterization and functionalization of P3HT-CNT nanocomposite thin films with doped Ag_2O", East Eur. J. Phys., (1), 342–354 (2024).DOI: 10.26565/2312-4334-2024-1-32.
[4] Q. Fu, P. Yang, X. Huang, et al., "Rational molecular and device design enables organic solar cells approaching 20% efficiency. DOI: 10.1038/s41467-024-46022-3
[5] B. H. Mohammed and E. T. Abdullah, "Comparison between horizontal and vertical OFETs by using poly(3-hexylthiophene) (P3HT) as an active semiconductor layer", Iraqi J. Sci., 61, 1040–1050 (2020). DOI: 10.24996/ijs.2020.61.5.13
[6] F. Laquai, D. Andrienko, R. Mauer, and P. W. M. Blom, "Charge carrier transport and photogeneration in P3HT:PCBM photovoltaic blends", Macromol. Rapid Commun., 36(11), 1001–1025 (2015). DOI: 10.1002/marc.201500047
[7] L.Rodrigues Koenig, et al., "Effects on the emission of different interfaces formed between poly(3-methylthiophene) and poly(3-octylthiophene): Electrochemical impedance and photoluminescence spectroscopy studies", Heliyon, 8, e09515 (2022). DOI: 10.1016/j.heliyon.2022.e09515
[8] S. Kang, T. W. Yoon, G.-Y. Kim, and B. Kang, "Review of conjugated polymer nanoparticles: from formulation to applications", ACS Appl. Nano Mater., 5, (2022). DOI: 10.1021/acsanm.2c04730
[9] M. Mcoyi, K. Mpofu, M. Sekhwama, and P. Mthunzi-Kufa, "Developments in localized surface plasmon resonance", Plasmonics, (2024). DOI: 10.1007/s11468-024-02620-x
[10] M. A. Mustafa and E. T. Abdullah", Iraqi J. Phys., 17, 122–127 (2019). DOI: 10.30723/ijp.v17i43.490
[11] R. Gan, D. Duleba, R. P. Johnson, and J. H. Rice, "p-Type organic semiconductor–metal nanoparticle hybrid film for the enhancement of Raman and fluorescence detection", J. Phys. Chem. C, 129, 3659–3666 (2025). DOI: 10.1021/acs.jpcc.4c08030
[12] A. Kasus-Jacobi, J. L. Washburn, C. A. Land, and H. A. Pereira, "The photosensitive activity of organic/inorganic hybrid devices based on Aniline Blue dye: Au nanoparticles (AB@Au NPs)", Sensors and Actuators A: Physical, 330, 112856 (2021). DOI: 10.1016/j.sna.2021.112856
[13] R. Abbas, J. Luo, X. Qi, A. Naz, I. A. Khan, H. Liu, S. Yu, and J. Wei, "Silver nanoparticles: synthesis, structure, properties and applications", Nanomaterials, 14, 1425 (2024). DOI: 10.3390/nano14171425
[14] D. Zhang, Z. Li, and K. Sugioka, "Femtosecond laser fabrication in transparent materials", J. Phys. Photonics, 3, (2021).
[15] I. Y. Khairani, G. Mínguez-Vega, C. Doñate-Buendía, and B. Gökce, "Ultrafast laser synthesis of nanoparticles in liquids: Mechanisms and strategies", Phys. Chem. Chem. Phys., 25, 19380–19408 (2023).
[16] F. Abd alahadi, N. S. Shnan, and S. F. Haddawi, "Enhancement surface plasmon resonance in the visible region by different active media", Journal of Nanostructures, 14(1), 184–194 (2024). DOI: 10.22052/JNS.2024.01.019
[17] M. I. Rahmah, A. M. Ahmed, T. M. Al-Rashid, and A. J. Qasim, "Preparation of silver nanoparticles using laser ablation for in vitro treatment of MCF-7 cancer cells with antibacterial activity", Plasmonics, 19(4), 2097–2105, 19(4), (2024). DOI: 10.1007/s11468-023-02150-y
[18] H. Kaçuş, M. Biber, and Ş. Aydoğan, "Role of Au and Ag nanoparticles on organic solar cell based on P3HT:PCBM active layer", Appl. Phys. A, 126, 817 (2020). DOI: 10.1007/s00339-020-03992-7
[19] P. Muenraya, S. Sawatdee, T. Srichana, and A. Atipairin, "Silver nanoparticles conjugated with colistin enhanced the antimicrobial activity against Gram-negative bacteria", Molecules, 27, 5780 (2022). DOI: 10.3390/molecules27185780
[20] H. Kaçuş, Ö. Metin, M. Sevim, M. Biber, A. Baltakesmez, and Ş. Aydoğan, "A comparative study on the effect of monodisperse Au and Ag nanoparticles on the performance of organic photovoltaic devices", Opt. Mater., 116, 111082 (2021).
[21] I. M. Ibrahim, "Synthesis and characteristics of Ag, Cu/Au core/shell nanoparticles produced by pulse laser ablation", Iraqi Journal of Science, 58(3C), 1651-1659 (2021).

[22] R. Gan, D. Duleba, R. P. Johnson, and J. H. Rice, "p-Type organic semiconductor–metal nanoparticle hybrid film for the enhancement of Raman and fluorescence detection", J. Phys. Chem. C, 129, 3659–3666 (2025). DOI: 10.1021/acs.jpcc.4c08030.
[23] Y. Zhao, K. Zheng, J. Ning, T. Xu, and S. Wang, "Plasmonics in organic solar cells: toward versatile applications", ACS Appl. Electron. Mater., 5, 632–641 (2023). DOI: 10.1021/acsaelm.2c01607
[24] A. A. Hussein, A. A. Sultan, M. T. Obeid, A. T. Abdulnabi, and M. T. Ali, "Synthesis and characterization of poly(3-hexylthiophene)", Int. J. Sci. Eng. Appl. Sci., 1, (2015).
[25] J. Zhang, Y. Huang, Y. Dan, and L. Jiang, "P3HT/Ag/TiO_2 ternary photocatalyst with significantly enhanced activity under both visible light and ultraviolet irradiation", Appl. Surf. Sci., 488, 228–236 (2019). DOI: 10.1016/j.apsusc.2019.05.150
[26] B. Hajduk, P. Jarka, H. Bednarski, et al., "Thermal and optical properties of P3HT:PC70BM:ZnO nanoparticles composite films", Sci. Rep., 14, 66 (2024). DOI: 10.1038/s41598-023-47134-4
[27] E. K. Salman and G. S. Muhammed, "Study of some structural and optical properties for synthesized graphene/polyaniline/ZnS nanocomposite", Iraqi J. Phys., 22(4), 53–66 (2024). DOI: 10.30723/ijp.v22i4.1244

جسيمات نانوية فضية مُزالة بالليزر ومُضمنة في P3HT: دراسة للتحسين الهيكلي والبصري

زينب عبد الكريم* ،استبرق طالب عبدالله

قسم الفيزياء، كلية العلوم، جامعة بغداد، بغداد، العراق

البريد الالكتروني للباحث:zainab.jabbar1804a@sc.uobaghdad.edu.iq

الخلاصة :تعتبر طبقات نقل الثقوب هي مكونات أساسية للأجهزة القائمة على الموصلات العضوية. تُعد الجسيمات النانوية المعدنية (NPs) مواد ممتازة لهذا الغرض. تصف هذه الورقة البحثية تحضير جسيمات نانوية فضية (Ag NPs) باستخدام طريقة الليزر، والتي خُلطت بعد ذلك مع البوليمر العضوي بولي (3-هكسيل ثيوفين) (P3HT) بتركيزات مختلفة (0.1، 0.3، و0.4٪ وزنًا). دُرست البنية والبنية والخصائص البصرية للمركب النانوي الجديد باستخدام حيود الأشعة السينية (XRD)، ومجهر مسح إلكتروني بانبعاث المجال (FESEM)، ومجهر القوة الذرية (AFM)، ومطيافية الأشعة فوق البنفسجية-المرئية. أظهرت بيانات حيود الأشعة السينية أن جسيمات النانو الفضية المُنتجة لها بنية بلورية، حيث تُرى أقوى القمم عند زوايا 38.1 درجة، 44.3 درجة، 64.4 درجة، و77.4 درجة. أظهرت اختبارات FESEM و AFM أن وجود المزيد من جسيمات النانو الفضية يجعل السطح أكثر خشونة ويساعد على نشر الجسيمات النانوية بشكل أفضل حيث زادت خشونة السطح من 2.04 إلى 2.46 نانومتر، وتغير متوسط خشونة الفيلم (Ra) من 1.55 إلى 1.81 نانومتر، وتراوح أقصى ارتفاع للفيلم (Rmax) من 22.34 إلى 25.38 نانومتر. أظهرت نتائج مطيافية الأشعة فوق البنفسجية والمرئية أن المادة تمتص المزيد من الضوء بسبب تأثير رنين البلازمون السطحي الموضعي (LSPR)، مما تسبب في انتقال قمم الامتصاص إلى أطوال موجية أقصر وخفض فجوة الطاقة الضوئية من 2.1 إلكترون فولت لـ P3HT النقي إلى 2 إلكترون فولت بتركيز 0.3٪ وزني من جسيمات النانو الفضية. تتميز مركبات P3HT النانوية مع جسيمات النانو الفضية ببنية وخصائص بصرية أفضل، مما يجعلها مثالية للخلايا الشمسية العضوية والتطبيقات الإلكترونية .